SUPPLEMENTARY DATA

Subjects inclusion/exclusion criteria

Inclusion criteria were: (i) age = 18-65 years; (ii) BMI=25-40 kg/m^2; (iii) FPG = 100-125 mg/dl or HbA1c = 5.7-6.4%; (iv) 2-hour glucose concentration above 140mg/dl after 75g glucose load, i.e., having impaired glucose tolerance or newly diagnosed type 2 diabetes. Exclusion criteria included: (i) previous treatment with medications known to affect glucose metabolism (ii) blood pressure > 140/90 mmHg; (iii) serum creatinine > 1.6 mg/dl; (iv) hematocrit < 35%, (v) evidence of major organ system disease as determined by medical history, physical exam, and routine screening blood chemistries.

Positron Emission Tomography

PET Scanner: Scanning was performed using a Siemens/CTI HR+ scanner (Siemens, Inc, Knoxville, TN) which is a 63-slice, high-sensitivity, high-resolution (4.1 mm in 3D mode) whole body scanner capable of 2D and 3D data acquisition. The sensitivity of the scanner at the center of field of view is 5.24 cps/kBq in 2D and 36.57 cps/kBq in 3D mode.
PET Imaging: The position of the subject was optimized in the scanner in order to scan the heart and a 20-min transmission scan was obtained after exposure of a retractable ^{68}Ge ring source to correct all subsequent emission data for tissue attenuation of γ-photons. Then, all subjects received an intravenous injection of 185 ± 37 MBq (5 mCi) of ^{18}F-FDG, while lying supine on the scanner bed at T=0. At the same time of the injection of ^{18}F-FDG subjects consumed a flavored drink containing 75 grams of glucose while lying in the supine position. At T=0 minutes a 60 minute dynamic scan was obtained to image the heart (34 frames, 12 x 120, 6 x 180, 5 x 300, 4 x 600, 6 x 1800, 1 x 600 s). At T=60 minutes the PET scanner was focused on the head. A transmission scan of the brain to serve as attenuation correction map and anatomic reference was performed and followed by 2D dynamic imaging (6 frames of 300 seconds each), and then by a 10-minute static 3D scan. Arterialized blood samples were collected throughout the scan to measure whole blood and plasma ^{18}F-FDG radioactivity over time.

Image Processing: Initially, each subject's brain PET images were spatially normalized to support the use of standard ROI. Thus, brain images were registered within the Talairach brain space to properly label the anatomical brain areas. This was a two-step process in which low-resolution PET images were aligned with high-resolution anatomical MR images of reference and MR images were aligned with the high-resolution brain template. Alignment transforms for the PET images (PET-to-MRI) were concatenated with those of the MR images (MRI-to-Talairach) to register the PET images in Talairach space. Linear affine transforms were used for alignment (1). Standard regions of interest defined in Talairach space were then used to analyze regional ^{18}F-FDG levels within the registered PET images. The primary focus of the study was on cortical and subcortical grey-matter regions of the brain. Brain ROIs were drawn in the nucleus of solitary tract, brainstem, insula, putamen, caudate, amygdala, limbic system, hypothalamus, orbitofrontal lobe, thalamus, and the anterior and posterior cingulate cortices. In addition, 2 main ROIs were defined to pool brain regions/nuclei involved in specific and similar brain functions: (i) glucose homeostasis regulation areas comprised of the nucleus of solitary tract, brainstem, insula, putamen, caudate, amygdala, limbic system and hypothalamus, and (ii) food reward system comprised of orbitofrontal lobe, thalamus, anterior and posterior cingulate, putamen, caudate, amygdala and limbic system.

Regional analysis was performed using the ROI analysis tool implemented in the Java-3D based program Mango developed by one of the authors (1) (http://ric.uthscsa.edu/mango/). Each ROI was further optimized in terms of boundary accuracy using morphological operations. For each brain region

evaluated, the ROI was drawn with the same volume in EX and PLC scans for each participant to allow comparison between treatments and to evaluate the effect of EX on ^{18}F-FDG levels.
Radioactivity concentrations, measured in arterialized plasma samples over time, were used as the input function for calculations of brain glucose uptake, as detailed below. These were integrated by image-derived blood activity data in the first few minutes after injection. Regions of interest (ROI) were drawn in the left ventricular chamber of the heart for the measurement of radioactivity in arterial blood; special attention was paid to avoiding contamination from surrounding myocardial tissue. Image-derived blood values over time were converted into plasma concentrations using the hematocrit, according to Phelps et al. (2). Later points of the curve were corrected for spillover by *in vitro* measurement of arterialized plasma radioactivity.

Calculation of brain glucose uptake rate using a modified Gjedde-Patlak analysis

The Gjedde-Patlak plot is a model-independent approach that enables one to calculate of the net transfer rate K_i (influx constant), independent of the number of compartments (3-5), Figure A1. For brain studies the net transfer rate K_i (influx constant) is often calculated using a few time frames from the later times assuming that equilibrium is achieved and the relationship is linear (6).

Supplementary Figure A1. Two-compartment model by Patlak et al (4) where Cp represents plasma ^{18}F-FDG radioactivity, Ct is the tissue radioactivity, and Ki (min^{-1}) is the fractional uptake rate.

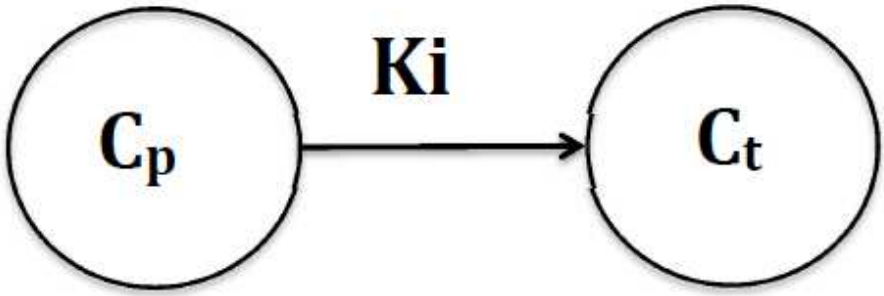

The Gjedde-Patlak plot has the integral of the blood ^{18}F-FDG concentration from time 0 to t min (kBq × min/ml) normalized by blood ^{18}F-FDG concentration on the X axis vs. brain tracer concentration (for example from 60-90 min (kBq/ml) normalized by blood ^{18}F-FDG concentration at time t on the Y axis:

$$\frac{Ct(t)}{Cp(t)} = \mathrm{Ki} \cdot \frac{\int_0^t Cp(z)\,dz}{Cp(t)} + \text{const.} \qquad \text{equation A1}$$

where *Ct* and *Cp* are tissue and plasma radioactivity levels at each sampling time point (*t*).
The slope of the linear phase represents the fractional uptake rate (Ki, min−1), i.e., K_i represents the amount of accumulated tracer in relation to the amount of tracer that has been available in plasma.
The Gjedde-Patlak analysis was developed to measure tissue glucose uptake of FDG under conditions of constant plasma glucose concentrations, either during fasting or during a hyperinsulinemic euglycemic or hyperglycemic clamp. The brain glucose uptake rates (CMR_{glu} expressed in μmol/min per ml of tissue) are obtained by multiplying times the plasma glucose concentration (G(t)) divided by appropriate lumped constant (LC=0.81) (7):

SUPPLEMENTARY DATA

$$CMR_{glu} = K_i * meanG(t)/LC \qquad \text{equation A2}$$

However, this does not take into account possible changes in blood glucose concentration during the period before starting brain image acquisition (i.e., from 0-60min).

In this set of experiment, we infused the same dose of FDG under two different conditions (ie during exenatide or placebo injection 30 min before administration of ^{18}F-FDG) that generated different changes in plasma glucose and insulin concentrations but similar systemic rates of glucose disposal (See Figure A2).

Supplementary Figure A2. Panel A: plasma ^{18}F-FDG Concentration Following Acute IV Administration. Plasma glucose (Panel B) and insulin (Panel C) concentrations and systemic glucose disposal (Panel D) during the first 60 min after FDG bolus and oral glucose ingestion are displayed.

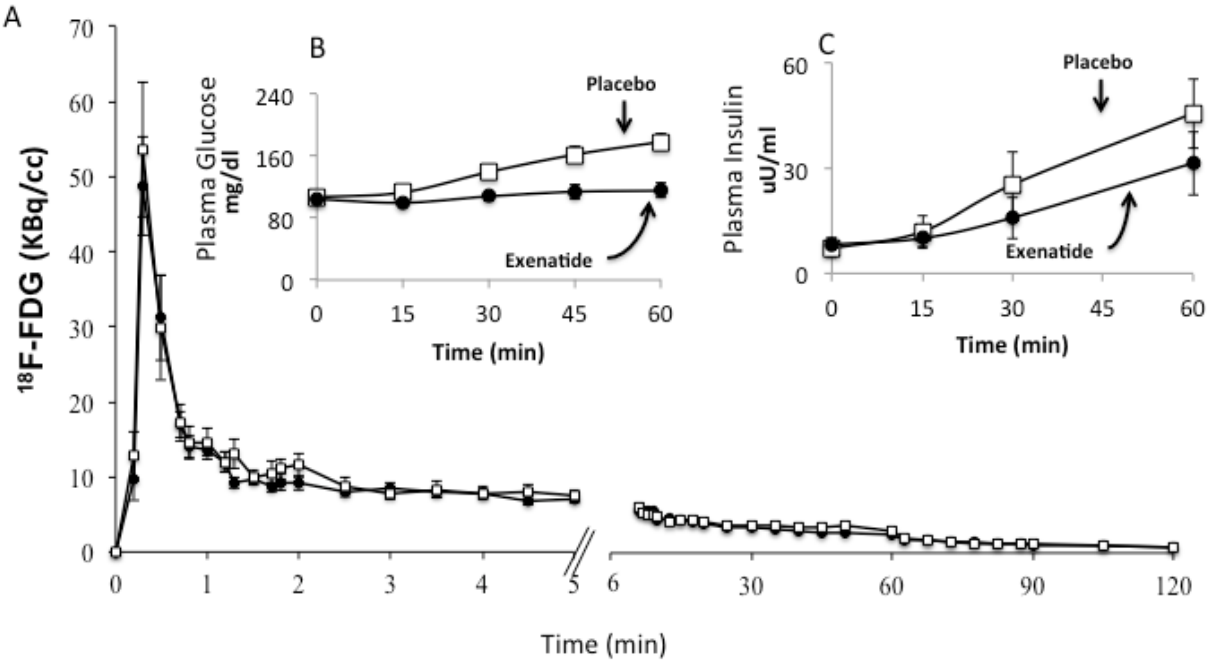

When glucose concentrations are changing several approaches have been used (8). The previously proposed methods multiply Ki times the average glucose concentration. Since changes in plasma glucose concentration were time dependent and different in placebo vs. EX studies, this approach did not account for real tracer/tracee competition. The great majority of ^{18}F-FDG clearance occurred during the first 5-10 min after ^{18}F-FDG injection, when plasma insulin and glucose concentrations were not different from baseline and were superimposable in both studies. Higher plasma glucose concentrations in the placebo versus Exenatide group were observed only after 30 minutes of FDG injection. This allows one to hypothesize that substrate competition was similar in the two studies during the first 5-10 min, when most of ^{18}F-FDG disappeared from the plasma, while after 30 minutes a higher glucose concentration in the placebo group could lead to reduced tissue FDG uptake. This is justified by the fact that during both studies systemic Rd was similar and not substantially different from baseline (figure 3), due to small changes in the plasma insulin concentration.

SUPPLEMENTARY DATA

In order to account for substrate competition and differences in glucose concentrations we used a modified Gjedde-Patlak plot based on the integral of plasma specific activity (SA(t)=Cp(t)/G(t)) (equation A3) rather than a plot based on the plasma FDG concentration (equation A1)

$$\frac{Ct(t)}{Cp(t)} = \mathrm{Ki} \cdot \frac{\int_0^t SA(z)\,dz}{Cp(t)} + \mathrm{const.} \qquad \text{equation A3}$$

where K_i represents the tissue uptake rate (μmol/min per ml of tissue). CMR_{glu} was then calculated as K_i divided by appropriate lumped constant (LC=0.81, equation A4):

$$CMR_{glu} = K_i / LC \qquad \text{equation A4}$$

Please note that equation A3 is similar to the formula previously proposed and validated by Dunn et al (5).

We tested and verified that the modified Gjedde-Patlak plot was linear (see in figure A3 an example plot from one subject). The slope of the plot, i.e. the new Ki, is the brain tissue glucose uptake rate (expressed in μmol/min per ml of tissue)

Supplementary Figure A3. Linear relationship between tracer concentration in tissue and integral of plasma specific activity normalized by tracer plasma glucose concentration in one study subject.

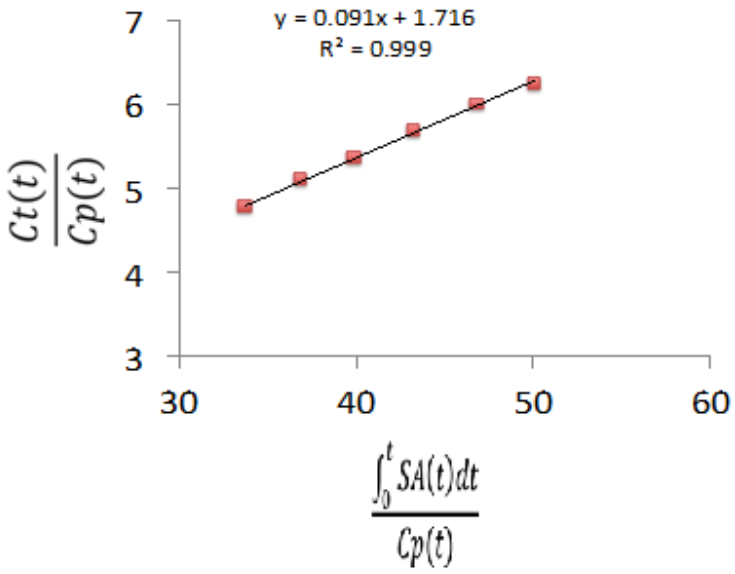

SUPPLEMENTARY DATA

References

1. Lancaster JL, Laird AR, Eickhoff SB, Martinez MJ, Fox PM, Fox PT: Automated regional behavioral analysis for human brain images. Front Neuroinform 2012;6:23
2. Phelps ME, Huang SC, Hoffman EJ, Selin C, Sokoloff L, Kuhl DE: Tomographic measurement of local cerebral glucose metabolic rate in humans with (F-18)2-fluoro-2-deoxy-D-glucose: validation of method. Ann Neurol 1979;6:371-388
3. Gjedde A: High- and low-affinity transport of D-glucose from blood to brain. J Neurochem 1981;36:1463-1471
4. Patlak CS, Blasberg RG, Fenstermacher JD: Graphical evaluation of blood-to-brain transfer constants from multiple-time uptake data. J Cereb Blood Flow Metab 1983;3:1-7
5. Patlak CS, Blasberg RG: Graphical evaluation of blood-to-brain transfer constants from multiple-time uptake data. Generalizations. J Cereb Blood Flow Metab 1985;5:584-590
6. Varrone A, Asenbaum S, Vander Borght T, Booij J, Nobili F, Nagren K, Darcourt J, Kapucu OL, Tatsch K, Bartenstein P, Van Laere K, European Association of Nuclear Medicine Neuroimaging C: EANM procedure guidelines for PET brain imaging using [18F]FDG, version 2. European journal of nuclear medicine and molecular imaging 2009;36:2103-2110
7. Wienhard K: Measurement of glucose consumption using [(18)F]fluorodeoxyglucose. Methods 2002;27:218-225
8. Dunn JT, Anthony K, Amiel SA, Marsden PK: Correction for the effect of rising plasma glucose levels on quantification of MR(glc) with FDG-PET. J Cereb Blood Flow Metab 2009;29:1059-1067